Available online at www.sciencedirect.com
SCIENCE DIRECT®
Journal of Magnetic Resonance 177 (2005) 146–151
JMR Journal of Magnetic Resonance
www.elsevier.com/locate/jmr

Retrieval of transverse relaxation time distribution from spin-echo data by recurrent neural network

R.C.O. Sebastião, J.P. Braga *

Departamento de Química, ICEx, Universidade Federal de Minas Gerais, (31270-901) Belo Horizonte, MG, Brazil

Received 25 April 2005; revised 18 July 2005

Abstract

Inversion of transverse relaxation time decay curve from spin-echo experiments was carried out using Hopfield neural network, to obtain the transverse relaxation time distribution. The performance of this approach was tested against simulated and experimental data. The initial guess, necessary for the integration procedure, was established as the analytical Laplace inversion. Together with errors in the simulated data, inversion was also carried out with errors in this initial guess. The probability density function, calculated by the neural network, is used in multiple sclerosis diagnostics.

Keywords: Relaxation; Ill-posed; Neural network; Spin-echo; Inverse problem

1. Introduction

The first spin-echo experiment was carried out by Hahn in 1949 [1,2], just after the nuclear magnetic resonance discovery. Inherent imperfections of the applied magnetic field, together with different nuclear magnetization at each infinitesimal volume element, imply a rapid decay of the free induction signal [3]. To circumvent this situation, multiple refocusing pulses can be applied, resulting in a train of spin echoes. This will enable the measurement of the spin–spin relaxation time. The time evolution of the nuclear magnetization, when the free motion is perturbed by two successive pulses, is called the Hahn echo phenomena.

The intensity of the peak in each spin-echo time can be used to calculate the transverse relaxation time by, for example, fitting the data to the smallest number of discrete exponential terms. This will produce a set of number, usually tabulated as the T_2 values. In the present work the spin-echo data will be used to recover, not only individual values of the relaxation time, but its distribution density function. This will provide useful information for the experimentalist, for this distribution can give important chemical information.

Quantitative interpretation of nuclear magnetic resonance data has been performed in [4–6] using the non-negative least square with constraints method and, also, using the Contin package [7]. In both these cases, the regularization parameter has to be determined. The non-negative least square with extra condition is, in fact, equivalent to the Tikhonov regularization [8] and the procedure to determine the free parameter has been discussed in [9].

Recovering the transverse relaxation time distribution from spin-echo data is, in fact, a problem known as ill-posed. The usage of recurrent neural network [10] has proved to be a powerful method to handle this kind of problem and has been applied to other situations in chemistry [11,12]. This approach is to be tested with simulated and experimental data for retrieving the transverse relaxation time distribution. Experimental data will be taken from magnetic resonance images in multiple sclerosis (MS) tissues [13].

* Corresponding author.
E-mail address: jpbraga@oxigenio.qui.ufmg.br (J.P. Braga).

1090-7807/$ - see front matter © 2005 Elsevier Inc. All rights reserved.
doi:10.1016/j.jmr.2005.07.017

2. Inverse problem and the spin-echo phenomena

Relaxation of the gyroscopic motion was defined by Bloch [14] in 1946 with the parameters T_1 and T_2

$$\frac{d\mathbf{M}}{dt} = \gamma(\mathbf{M}\times\mathbf{B}) - \frac{M_x\vec{i} + M_y\vec{j}}{T_2} - \frac{(M_z - M_0)\vec{k}}{T_1} \quad (1)$$

with $\mathbf{M}$ being the total magnetization vector, M_0 the equilibrium magnetization, and $\mathbf{B}$ the total magnetic field vector. This equation can be solved as a function of time for the transverse relaxation,

$$M_{xy} = M_0 \exp\left(\frac{-t}{T_2}\right). \quad (2)$$

In the same volume element there is no variation of the applied field intensity and the above equation is correct. Nevertheless, due to the spatial inhomogeneity, neighboring elements experiment slightly different applied fields and an important modification would be to introduce multiple T_2 components, resulting in a transverse magnetization equation [13,15]

$$M_{xy} = \sum P(\lambda_i)\exp(-t\lambda_i) \quad (3)$$

with $(\lambda_i = 1/T_2^{(i)})$ the rate constant for each process and $P(\lambda_i)$ its corresponding probability. Considering a continuous distribution of transverse relaxation time and the probability density function $f(\lambda) = P(\lambda)/\Delta\lambda$ [12], Eq. (3) can be re-written as,

$$\int_a^b K(t,\lambda)f(\lambda)\,d\lambda = g(t) \quad (4)$$

in which $g(t)$ is the signal intensity, measured at echo time t and $K(t,\lambda) = \exp(-t\lambda)$ is the kernel of the transformation.

Eq. (4) is a Fredholm integral equation of first kind [16] which, in general terms, can be interpreted as $f(\lambda)$ being an input, $K(t,\lambda)$ being an apparatus, and $g(t)$ an output. For a given $K(t,\lambda)$ and $f(\lambda)$ calculation of $g(t)$ is a simple problem, the direct problem. On the other hand, calculation of $f(\lambda)$ from $K(t,\lambda)$ and $g(t)$ is a much more complicated problem, being the inverse problem. Within a representation for the Fredholm integral equation, $\mathbf{Kf} = \mathbf{g}$ will be established, with $\mathbf{f}\in R^n$, $\mathbf{g}\in R^m$ and $\mathbf{K}\in R^{m\times n}$. In this framework, one can define an ill-posed problem as a problem in which one of the three conditions

1. for every $\mathbf{f}\in R^n$ there *exist* a $\mathbf{g}\in R^m$ such that $\mathbf{Kf} = \mathbf{g}$;
2. the solution of the problem, $\mathbf{f}$, is *unique* in R^n; and
3. the dependence of $\mathbf{f}$ with $\mathbf{g}$ is *continuous*;

is not satisfied [17]. Therefore, retrieval of transverse relaxation time distribution from spin-echo data is an ill-posed problem and requires special techniques for its solution. The two most popular techniques to solve an inverse ill-posed problem are the Tikhonov regularization [8] and the singular value decomposition method [12,18]. A third method, the Hopfield recurrent neural network, proves to be more powerful than these two methods.

3. Hopfield neural network

The Hopfield neural network is a single recurrent layer network with logic units fully connected. The state of the neurons, u_i, is calculated by an activation function formed by the weighted sum of all its inputs [10,11]. Increasing functions of the state of the neurons, i.e., $\partial f/\partial u > 0$, has to be chosen as transfer functions to satisfy the nervous impulse model [10].

Within this approach one may define an energy function,

$$E = \frac{1}{2}\sum_{j=1}^{m} e_j^2 = \frac{1}{2}\sum_{j=1}^{m}\left(\left(\sum_{i=1}^{n} K_{ij}f_i\right) - g_j\right)^2 \quad (5)$$

with $e_j = (\sum_i K_{ij}f_i) - g_j$, $f_i = \phi(u_i(t))$, n the number of points used to represent Eq. (4) and m, the number of available data. Considering this energy function, the stable state $\mathbf{f} = [f_1 f_2 \cdots f_n]$ that minimizes $\|\mathbf{Kf} - \mathbf{g}\|_2^2$ is reached since the Hamiltonian relation

$$\frac{du_i}{dt} = -\frac{\partial E}{\partial f_i} \quad (6)$$

is imposed. In this way, the time evolution of the outputs of the neurons is given by

$$\frac{du_i}{dt} = \sum_{j=1}^{n} T_{ij}f_j + I_i \quad (7)$$

with $T_{ij} = -\sum_{l=1}^{n} K_{li}K_{lj} = T_{ji}$ and $I_i = \sum_{j=1}^{n} K_{ji}g_j$.

This equation was integrated by a Runge–Kutta–Fehlberg method [19] until an establishment of the equilibrium, which corresponds to a solution $\mathbf{f}$ of the problem. The multiple solution character of the ill-posed problem can be observed along the integration. If the output error is within the experimental error, the experimentalist can decide the right solution, based, for example, on the relative areas and position of the components.

4. Multiple sclerosis background

Multiple sclerosis is a brain disease characterized by an abrupt onset of neurological symptoms [13,20,21]. The disease process starts with the lymphocytes attacking the myelin sheath around the axons in the white matter. The bilayer myelin sheath is composed principally of lipids and other support proteins. The stages of MS lesions mainly occur with, at first, the breaking down of the blood–brain barrier and entering of lymphocytes

into the extra cellular space resulting in an inflammation. Then, inflammation is decreased and there is significant loss of myelin and oligodendrocytes.

Contrast mechanism in magnetic resonance of images can be used to detect the inflammation in MS lesions. Therefore, a train of multiple spin-echo images can distinguish more completely MS lesions from the normal white matter using the T_2 relaxation properties [4,5]. The spins enclosed by the tissues present an effective spin–spin interaction and dephase faster ($T_2 \approx$ tens of milliseconds), because each isochromat is affected by the local magnetic field of the neighboring spins. On the other hand, variations in local magnetic field of the freely moving spins decreases the spin–spin interaction importance, with a relatively slower dephasing ($T_2 \approx$ seconds) [22]. Therefore, the water in tissues with MS lesions has intrinsic increased transverse relaxation times in comparison with the surrounding white matter [5]. This information is important to quantify the distribution function obtained by the inversion procedure.

5. Results and discussion

5.1. Analysis with simulated data

The signal intensity, $g(t)$, measured at echoes time, t, can be expressed by the Laplace transform of the probability density function, $f(\lambda)$, as in Eq. (4). The first part of this work was performed using simulated data to verify the efficiency of the method. To represent the experimental T_2 decay curve [13], a bi-exponential function was proposed as a model,

$$g(t) = \sum_{i=1}^{2} A_i \exp(-\alpha_i t). \tag{8}$$

The constant A_i was determined by the amplitude of the T_2 decay curve and α_i as the rate constant for each component. Normalized simulated data are in fair agreement with the published data [13]. The result is presented in Fig. 1 and the necessary constants in Table 1.

To calculate the T_2 distribution one can try to find the inverse matrix $\mathbf{K}^{-1}$, if the number of available data coincides with the representation size. However, $\mathbf{K}$ is an ill-conditioned matrix resulting in an inverse with large values compared with the original values of $\mathbf{K}$. Any small error in the data is sufficient to amplify the solution, if it is computed as $\mathbf{K}^{-1}\mathbf{g}$. This non-continuity in the data with respect to the solution is sufficient to classify the inversion of data in spin-echo experiments as an ill-posed problem.

The system of differential equations, Eq. (7), requires an initial condition to be solved. The quality of this initial condition is an important aspect of the neural network procedure and is responsible for better results with less computational time. In this sense, the $f(\lambda)$ function for initial guess, used for the simulated and experimental data, was calculated by the inverse Laplace transform [23,24],

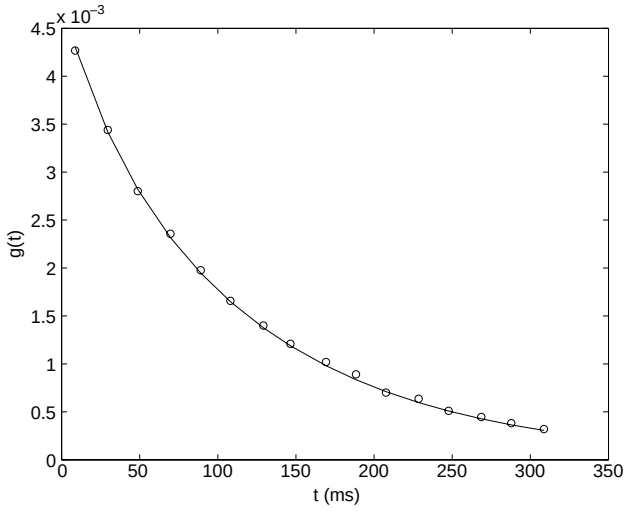

Fig. 1. Experimental (○) and simulated (full line) data for multi-spin-echo experiment.

Table 1
Parameters for the density function, Eq. (8)

Variables	Values
A_1	850
A_2	150
α_1	1/120 ms^{-1}
α_2	1/30 ms^{-1}

$$f(\lambda) = \lim_{k\to\infty}\left(\sum_{i=1}^{2}\frac{(-1)^{2k}}{k!}\alpha_i^k A_i \exp(-\alpha_i k/\lambda)\left(\frac{k}{\lambda}\right)^{k+1}\right). \tag{9}$$

The constants A_i and α_i are the same as in Eq. (8) whereas λ is the inverse of the transverse relaxation time. Numerical integration of the direct problem, with $k = 30$ in Eq. (9), was performed generating synthetic data with seven significant figures.

The matrix of $\mathbf{Kf} = \mathbf{g}$ problem was calculated in a rectangular representation [25] with $n = 32$ and 16 experimental points. This base size was tested analyzing if the residual error $\|\mathbf{Kf} - \mathbf{g}\|_2^2$ is within the experimental error. The total of eight significant figures was reached.

Two important properties of the recurrent neural network have to be emphasized at this point. One is related with the decreasing character of the energy function. For any initial condition $\frac{dE}{dt} < 0$, that is, the final result will always be better than the initial guess. The second property refers to the initial condition. If the initial guess is the exact solution, $\frac{du_i}{dt} = 0$, a result which can be seen from Eq. (6). These two properties were tested numerically and the recovered result from Eq. (9) as initial guess is presented in Fig. 2.

Errors up to 30% were considered in the initial guess. This was achieved by multiplying the initial guess by a factor. For all these situations, summarized in Table 2, the neural network presents two peaks with residual error smaller than the one in the initial guess.

Another analysis was made including 20% of error in the simulated data of the T_2 decay curve, presented also in Table 2. In this case, despite the solution presents negative values, the two peaks could also be recovered. At this point it is important to emphasize the solution obtained by the recurrent neural network has a smaller residual error when compared with the initial guess. Table 2 exemplifies the decreasing energy property of the present approach for the considered cases.

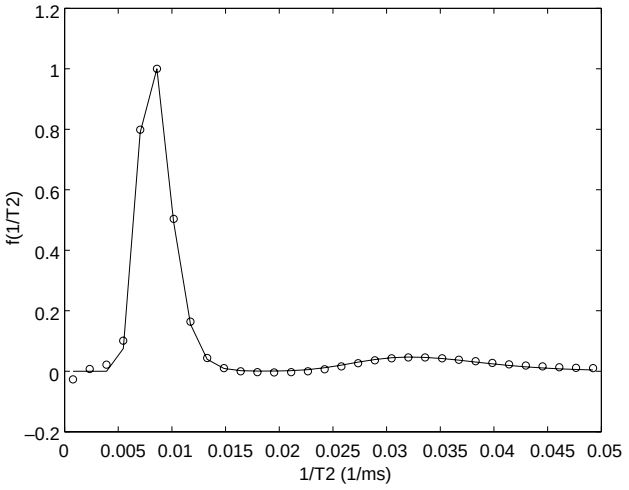

Fig. 2. Initial inverse Laplace guess (full line) and converged neuron states (○) for simulated data.

Table 2
Inverse Laplace transform and neural network residual errors

Inverse Laplace transform error $\|\mathbf{Kf}-\mathbf{g}\|_2^2$	Initial guess (%)	Neural network error $\|\mathbf{KV}-\mathbf{g}\|_2^2$
Simulated data		
1.456(−8)	0	1.946(−12)
	10	3.866(−12)
	20	5.166(−12)
	30	6.717(−12)
20% percentual error in simulated data		
2.5559(−6)	0	2.261(−6)
	10	2.261(−6)
	20	2.261(−6)
	30	2.261(−6)
Experimental data		
3.151(−8)	0	5.026(−9)
	10	5.039(−9)
	20	5.046(−9)
	30	5.053(−9)

The function **f** is the solution from the inverse Laplace transform method and **V** is the neural network response. Number in parenthesis are for power of 10.

5.2. Inversion of experimental data

Considering experimental data and the inverse Laplace transform function, Eq. (9), as initial guess, the neural network approach recovers an excellent transverse relaxation time distribution, as in Fig. 3. In this case errors up to 30% were also added in the initial guess, resulting a T_2 time distribution retrieval with two peaks, although, in some case, negative values can also be presented. To avoid these negative values, an appropriated filter can be used while treating with experimental data [26,27].

A sensitivity analysis of the neural network performance, with respect to the amplitude and rate constant, was carried out. The inverted results are not sensitive to the amplitudes. Although the neural network is sensitive to variations in the rate constant, a variation of 10% in this parameter gives tolerable results, as shown in Fig. 4.

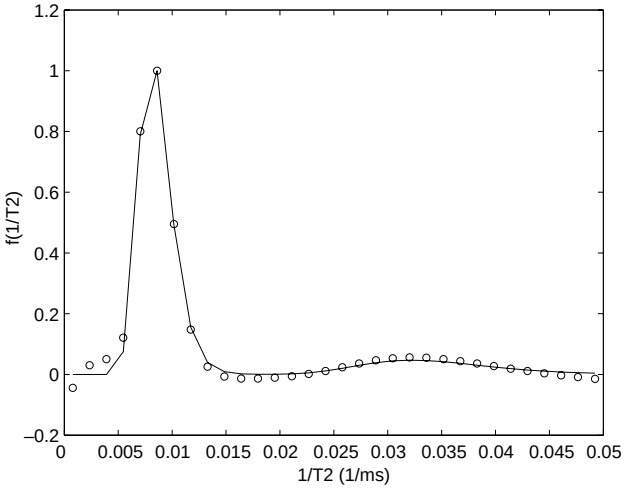

Fig. 3. The same as in Fig. 2 using experimental data.

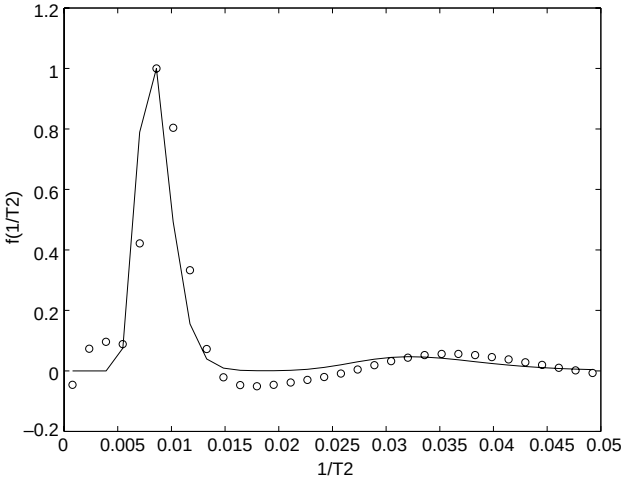

Fig. 4. Converged states of the neurons (○), using experimental data. The initial guess given to the network (full line), with 10% error in each of the parameters A_i and α_i ($i = 1,2$) in Eq. (9).

From the previous discussion it is clear that, although the solution using the inverse Laplace might contain the decaying rates and is a good initial guess, it can be considerable improved by using the recurrent neural network. This can be used to characterize and quantify, throughout the peak areas, a MS lesion tissue.

Integration of Eq. (7) was interrupted at a point in which the residual error $\|\mathbf{KV}-\mathbf{g}\|_2^2$, with V being the neural network response, reaches a desired tolerance. This was achieved, in average, for the maximum integration time of about 10^8 units.

5.3. Testing the initial condition

The previous results, based on the inverse Laplace transform as initial guess, is not taken to imply this constitutes a bias in the present method. To explore the robustness of the present approach the number of exponential in the initial condition will be given in such a way that it will not correspond to the number of exponential in the model function. Different initial conditions, with one and three exponentials, will be used to investigate the response of the neural network in these situations.

The converged solution, for an initial guess consisting only of the first exponential in the model function, is given in Fig. 5. Considering simulated data, the residual error was $\|\mathbf{KV}-\mathbf{g}\|_2^2 = 2.999\times10^{-12}$. Even with this initial guess, the neural network was able to identify the second peak in the density distribution function. The same arguments are valid if the experimental data are used. In this case $\|\mathbf{KV}-\mathbf{g}\|_2^2 = 5.034\times10^{-9}$.

A third exponential was added to the previous inverse Laplace transform function with two exponential. This new exponential has a smaller intensity with respect to the second peak and is located to the right, with a rate of 50 ms. As before, the results gives the two peaks in the right position, a result similar to the one presented in Fig. 5. In this case the residual error is also small, $\|\mathbf{KV}-\mathbf{g}\|_2^2 = 3.041\times10^{-12}$ and $\|\mathbf{KV}-\mathbf{g}\|_2^2 = 5.034\times10^{-9}$ for the simulated and experimental data, respectively.

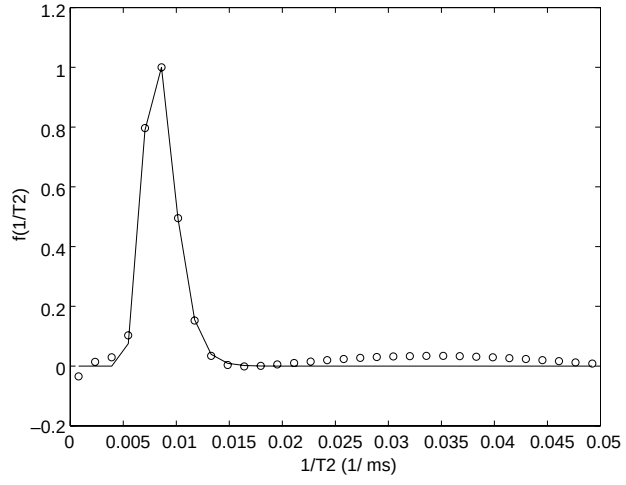

Fig. 5. Converged states of the neurons using simulated data. The initial guess given to the network has only the first exponential of Eq. (9). The solid line represents the initial guess and the circles the network response.

6. Conclusions

The inversion of multi-spin-echo experiment is an ill-posed problem, requiring some special techniques for its numerical treatment. The recurrent Hopfield neural network was chosen and the inversion procedure investigated with simulated and experimental data. The efficiency of the method was analyzed introducing errors and varying parameters in the initial guess.

The inverse Laplace transform as initial guess proved to be useful in the both case, with simulated and experimental data. The recurrent neural network, due to its property of decreasing energy, will improve the initial condition, generating a distribution function with lower residual error. For a initial guess, given by the inverse Laplace transform with a set of reasonable parameters, already known to MS lesions [13,15,22], the neural network will provide a distribution from the experimental data. The position and relative areas of the peaks can be analyzed quantitatively to MS lesion diagnostics.

The usage of the recurrent neural network for ill-posed problem is attractive for its efficiency and simplicity. The theory and numerical background requires only elementary concepts. For example, to understand basic equations, as Eq. (7), only simple concepts of calculus need to be introduced. Also, the computer code developed is very short. Except from the integration routine, the code has about 100 lines and is very simple to use. The methodology used here is not restricted to linear problems and has been extended also to non-linear problems [11]. Therefore, effects of non-linearity in magnetic resonance are possible to be studied by the recurrent neural network.

Acknowledgments

This work was supported by CNPq and FAPEMIG, Brazil.

References

[1] E.L. Hahn, An accurate nuclear magnetic resonance method for measuring spin–lattice relaxation times, Phys. Rev. 76 (1950) 145–146.
[2] E.L. Hahn, Nuclear induction due to free Larmor precession, Phys. Rev. 77 (1950) 297–300.
[3] D.M.S. Bagguley, Pulsed Magnetic Resonance: NMR, ESR and Optics, Clarendon Press, Oxford, 1992.

[4] K.P. Withall, Quantitative interpretation of NMR relaxation data, J. Magn. Reson. 84 (1999) 134–152.
[5] K.P. Withall, Investigation of analysis techniques for complicated NMR relaxation data, J. Magn. Reson. 93 (1991) 221–234.
[6] R.J.S. Brown, Uniform-penalty inversion of multiexponential decay data, J. Magn. Reson. 132 (1998) 65–77.
[7] C.H. Newcomb, S.J. Graham, M.J. Bronskill, Effects of nonlinear signal detection on NMR relaxation time analysis, J. Magn. Reson. 90 (1990) 279–289.
[8] A.N. Tikhonov, V. Arsénine, Solutions of ill-posed problems, Mir, Moscow, 1974.
[9] J.P. Braga, Numerical comparison between Tikhonov regularization and singular value decomposition methods using the L curve criterion, J. Math. Chem. 29 (2) (2001) 151–161.
[10] J.J. Hopfield, Neural networks and physical systems with collective computational abilities, Proc. Natl. Acad. Sci. USA 79 (1982) 2554–2558.
[11] R.C.O. Sebastião, N.H.T. Lemes, L.S. Virtuoso, J.P. Braga, Nonlinear global inversion of potential energy surfaces from the experimentally determined second virial coefficients, Chem. Phys. Lett. 378 (2003) 406–409.
[12] V.C. Viterbo, R.C.O. Sebastião, R.P.G. Monteiro, W.F. Magalhães, J.P. Braga, Probability density function from experimental positron annihilation lifetime spectra, J. Braz. Chem. Soc. 16 (1) (2005) 93–97.
[13] C.K. Jones, Quantitative Multi-component T_2 Analysis Using Fast Spin-Echo MRI, University of Western Ontario, London, 1997.
[14] F. Bloch, Nuclear induction, Phys. Rev. 70 (7–8) (1990) 317–334.
[15] R.S. Menon, P.S. Allen, Application of continuous relaxation time distributions to the fitting of data from model systems and excised tissue, Magn. Reson. Med. 20 (1991) 214–227.
[16] G.M. Wing, J.D. Zahrt, A primer on integral equations of first kind, SIAM, Philadelphia, 1991.
[17] J. Hadamard, Le probéme de Cauchy et les équations aux derivée partielle linéaires hyperboliques, Herman, Paris, 1932.
[18] S.J. Leon, Linear Algebra with Applications, sixth ed., Prentice-Hall, N.J, 2002.
[19] G.E. Forsythe, M.A. Malcolm, C.B. Moler, Computer methods for mathematical computations, Prentice-Hall, New Jersey, 1977.
[20] L. Steinman, The dynamics of multiple sclerosis: the charcot lecture, J. Neurol. 240 (1993) 28–36.
[21] F.W. Wessbecher, K.R. Maravilla, Multiple Sclerosis, second ed., Mosby Year Book, Missouri, 1992.
[22] H.W. Fischer, P.A. Rinck, Y.V. Haverbeke, R.N. Muller, Nuclear relaxation of human brain gray and white matter: analysis of field dependence and implications for MRI, Magn. Reson. Med. 16 (1990) 317–334.
[23] D.V. Widder, Advanced Calculus, second ed., Prentice-Hall, Englewood Cliffs, N.J., 1961.
[24] A.H. Deng, B.K. Panda, S. Fung, C.D. Beling, D.M. Schrader, Positron lifetime analysis using the matrix inverse Laplace transformation method, Nucl. Instr. Meth. B 140 (1998) 439–448.
[25] G.H. Golub, C.F. Van Loan, Matrix Computations, Johns Hopkins University Press, Baltimore, 1989.
[26] J.M. Bonny, O.B. Tanguly, M. Zanca, J.P. Renou, Multi-exponential analysis of magnitude MR images using a quantitative multispectral edge-preserving filter, J. Magn. Reson. 161 (2003) 25–34.
[27] V.C. Viterbo, J.P. Braga, A.P. Braga, M.B. de Almeida, Inversion of simulated positron annihilation lifetime spectrum using a neural network, J. Chem. Inf. Comput. Sci. 41 (2001) 309–313.